The role of bubble coalescence in Decompression Sickness

Mark Ransley

Supervisors: Umber Cheema & Nick Ovenden
University College London
m.ransley.12@ucl.ac.uk

Abstract

Coalescence - the formation of a larger bubble from the collision of two or more smaller ones - has been somewhat neglected in the study of Decompression Sickness (DCS), a condition where mathematical models are enabling breakthroughs in both its understanding and prevention. In this report we review the current literature on modelling DCS and bubble coalescence, and address the need and possible approaches for reconciling the two fields. We also experimentally investigate the effects of sodium chloride on bubble coalescence during the decompression of 3D collagen hydrogels.

Special thanks to Claire Walsh for providing critical shortcuts through the labyrinth of decompression literature, sharing many pages of valuable code and patiently guiding me through my first real lab session in *many* years.

I. Introduction

DECOMPRESSION SICKNESS or "the bends" is a form of dysbarism suffered by organisms undergoing changes in pressure, as the result of bubbles forming from metabolically inert gasses inside the body. Research into its prevention has been of much interest to the caisson engineering and aeronautical industries, though it is DCS in deep water SCUBA assisted diving that provides the motivation for this report.

As a diver descends, the ambient pressure increases due to the weight of the water above. This can be simply modelled as

$$p(z) = \rho g z + p_{atm} \tag{1}$$

where water has density ρ kg/m^3, z is the depth in metres, p_{atm} is the atmospheric pressure at the surface in pascals, and g is the gravitational strength, usually taken to be $9.81 m/s^2$.

This acts on various exposed air spaces around the body such as the chest, and thus breathing air must be supplied at the depth dependent pressure to counteract its effect on breathing. The high pressure gasses, mostly Nitrogen or, when Trimix[1] is breathed, Helium, become dissolved in the diver's blood, where they are carried around the body via perfusion (blood flow). Microbubbles then form, most likely within minuscule hydrophobic crevices [1], which subsequently migrate, accumulate and expand on ascent causing a plethora of unpleasant and threatening symptoms [2] [3]. Once contained in bubbles, the inert gasses become harder to eliminate [4].

However, a carefully planned ascent featuring "decompression stops" along the way can allow much of the dissolved gas to leave the body as partial pressures equilibrate - somewhat like the controlled opening of a fizzy drink - thus avoiding DCS. In response there has been a rich history of mathematical modelling associated with decompression, pioneered by the work of JS Haldane [5]. Dividing the body up into compartments based on their rates of gas uptake and release, Haldane presented the following equation for the time course of gas x's partial pressure in tissue T

$$\frac{dp_T^x}{dt} = \frac{p_a^x - p_T^x}{\tau_T} \tag{2}$$

where p_a is the atmospheric partial pressure and

$$\tau_T = \frac{L_T^x}{\dot{Q} L_b^x} \tag{3}$$

is the gas exchange time constant, a function of blood flow rate $\dot{Q}$ and solubility coefficients in tissue L_T and blood L_b.

Representing the body as a set of series and parallel compartments with associated partial pressure limits, algorithms by Haldane and later Workman and Bühlmann have been used to produce dive computers and tables with some success. However, such simple gas exchange models suffer a number of shortcomings including failure to account for repeated dives and other important factors such as exercise [5]. They also shed little light onto the still rather mysterious mechanisms behind DCS.

II. Bubble expansion in tissue

In static bubble modelling, the bubble may expand due to gas diffusing in from the environment as a result of differing partial pressures, and through gas 'evaporating in' from the surrounding liquid, termed the vapour pressure. It may collapse through the inverse of these processes, from the ambient pressure of its surrounding medium, and from surface tension forces acting on the interface. Thus for a bubble in equilibrium we have the Laplace equation [1]

$$p_i + p_v = p_{amb} + \frac{2\sigma}{R} \tag{4}$$

where R is the bubble's radius of curvature, and σ is the surface tension coefficient.

With multiple gasses, the partial pressure of each one is summed to give p_i, and it is commonplace to separate diffusible gasses, where partial pressures can be expected to evolve over time, from infinitely diffusible ones such as the

[1] For deep dives, Nitrogen gas can have intoxicating effects, so a Helium rich mixture is used.

metabolic gasses, where pressures may be assumed to equilibrate immediately. Solving (4) for R we obtain the critical radius R_c, a threshold below which the bubble will collapse.

For a diffusive gas x, the concentration can be described by

$$\frac{\partial c^x}{\partial t} = D^x \nabla^2 c^x \tag{5}$$

where D is the diffusion constant. Henry's law describes the relationship between concentration and partial pressure, and thus is essential for combining these equations. It is given as

$$c^x = \frac{L^x}{\mathcal{R}T} p^x \tag{6}$$

with temperature T and gas constant $\mathcal{R}$.

Gaseous pressure changes within the bubble come about through diffusion across the surface membrane, as described by the Fick equation

$$\frac{1}{\mathcal{R}T}\frac{d}{dt}(p_i^x V) = AD^x \left.\frac{\partial c^x}{\partial r}\right|_{r=R} \tag{7}$$

where R is the radius of the bubble (as opposed to the distance r from its centre), and V and A are the volume and surface area, given by

$$V = \frac{4\pi}{3}R^3 \qquad A = 4\pi R^2 \tag{8}$$

Given boundary conditions including initial bubbles with $R \geq R_c$ this system can be solved numerically together with the Haldane equation (2) using finite difference methods to yield expressions for growth and shrinkage of bubble radii over time at a given pressure and gas mixture. Numerical schemes and parameter values are given by O'Brien in [5].

There are a few differences in O'Brien's model; due to the non-aqueous medium, vapour pressure was not considered in (4), but instead there was a term for tissue elasticity, describing the tissue medium opposing the bubble volume. Also since O'Brien's research focused on a given volume of tissue rather than the body as a whole, (2) was not required.

A fairly recent set of NASA sponsored papers by Srinivasan *et al.* have considered ways of making the solutions more computationally tractable. The term 'well stirred' is used to describe tissue, or a region thereof, where diffusion does not occur due to the gases already being in equilibrium, and hence (5) can be set to zero leaving all environmental changes dependent on the perfusion term (2). Conversely, 'unstirred' regions must be equilibrated by diffusion. In [6] the group asked whether, for a single bubble, the model should consist of only two regions, bubble and unstirred but uniformly perfused tissue, or whether the unstirred region should be confined to a third boundary layer around the bubble, such that the remainder of tissue is well stirred (Fig. 1). The diffusion equation (5) was rewritten in terms of distance r from the bubble centre.

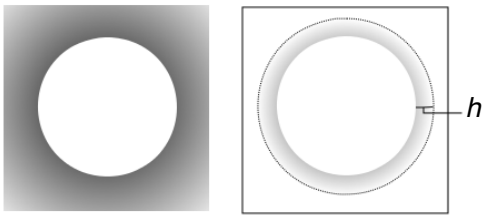

Figure 1: *Comparing the two region model (left) where diffusion affects the entire tissue beyond the bubble, and the three region (right), where diffusive effects are confined to a boundary layer of fixed width h.*

For both models, Srinivasan and colleagues used the quasi-static approximation - that is, assuming bubble dynamics occur on a far more rapid timescale than environmental pressure changes, so that $\partial p/\partial t$ may be set to zero. Subsequently they were able to obtain the following solutions for a single gas to the two and three region models respectively.

$$\frac{dR}{dt} = \frac{L_t D_t \left(\lambda + \frac{1}{R}\right)(p_t - p_i) - \frac{R}{3}\frac{dp_{amb}}{dt}}{p_{amb} + \frac{4\sigma}{3R}}$$

$$\frac{dR}{dt} = \frac{L_b D_t \left(\frac{1}{h} + \frac{1}{R}\right)(p_t - p_i) - \frac{R}{3}\frac{dp_{amb}}{dt}}{p_{amb} + \frac{4\sigma}{3R}}$$

where subscripts t and b represent the different solubilities of the gas in tissue and blood. Analogous solutions for multiple gases were

also provided. Evidently, the models are structurally very similar, however the two region model involves an infinite volume and thus is only applicable when the bubble to tissue size ratio is very large.

In [7] the group revised the model, noting that the three region model with fixed h violates Henry's law since, as the bubble expands, the volume of the boundary layer (and hence gaseous partial pressure) increases whilst the gas concentration does not. Thus, an expression for h was derived in terms of bubble volume, gas contents of both the bubble and tissue, and partial pressures such that Henry's law was obeyed.

In [8] the two region model was adapted to permit finite tissue volumes through variable perfusion, allowing for the tissue to again be eventually well stirred and hence finite in volume. This approach was generalised in [9] to allow for multiple bubbles. Interestingly, an expression was derived for the maximum number of bubbles a given volume could take, however unfortunately for this report coalescence effects were neglected.

These papers are by no means the extent of the tissue modelling literature, and indeed the models contained therein were based in part upon earlier ones discussed in more detail in the thesis of Michael Chappell [1], which focused largely on bubble nucleation during decompression. Chappell investigated the theory that bubbles are formed within hydrophobic crevices, most likely located in points of cellular contact and clefts between the endothelia of blood vessels. A range of crevice geometries were modelled, and simulations conducted to determine under what conditions bubbles may form and detach. It was suggested that the observed delay between a diver's ascent and the onset of DCS symptoms could be due to gas stored in bubbles being slowly released and then available for further nucleation, although the parameter values required for this are at the limits of the plausible ranges. However, importantly Chappell stated

"It is likely that the interaction between bubbles and the vasculature and other bubbles may introduce further time delays for the arrival of bubbles at observation sites."

Potential DCS related problems such as the occlusion of blood vessels are likely to require larger bubbles than those possible from decompression alone. Indeed, *in vivo* observation of decompression bubbles has in the past only been able to detect those $> 10\mu m$ in diameter [10], a figure only achieved in very aggressive simulated ascent profiles in O'Brien's model [5], where coalescence is assumed to occur instantaneously upon two bubbles making contact. However, the coalescence literature paints a more complicated picture.

III. Coalescence

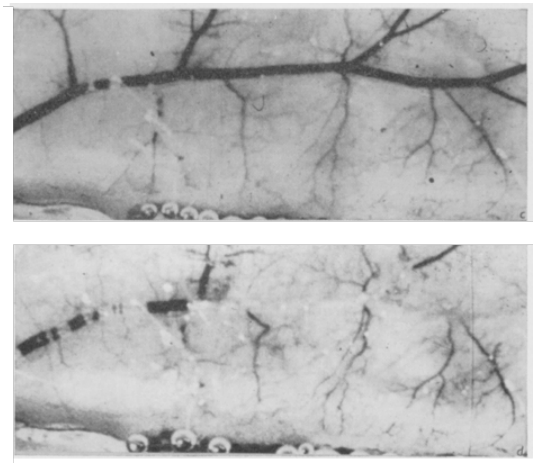

Figure 2: *Bubble coalescence observed in the veins of a mouse following decompression. Taken from Lever et al.*

In the simplest terms, the description of coalescence between two bubbles is stated in [12] among other works as:

1. Bubbles collide.
2. A small amount of the liquid between the bubbles is trapped and drains gradually.
3. The liquid film between the bubbles reaches a critical thickness and a film rupture occurs due to van der Waals forces, resulting in coalescence.

The value of critical thickness seems fairly stable from author to author; in [13] they claim

it to be 100Å, whilst in [14] it is claimed to be 5-10nm. Coalescence has been observed *in vivo* as a direct result of decompression (Fig. 2), though the modelling literature on this topic tends to be either purely academic in nature, or related to industrial processes, with little attention given to biological cases. In the static tissue models covered in Section II coalescence would occur due to the expansion of bubbles, yet in most scenarios collisions are the result of fluid motion as described by the Navier-Stokes equations for incompressible fluids:

$$\nabla \cdot \mathbf{U} = 0 \tag{9}$$

$$\rho \frac{D\mathbf{U}}{Dt} = -\nabla p + \nabla \cdot \mathbf{T} + \mathbf{f} \tag{10}$$

where $\mathbf{U}$ is the fluid velocity, $\mathbf{f}$ represents body forces, usually gravity (in which case $\mathbf{f} = \rho\mathbf{g}$), and $\mathbf{T}$ represents stress factors. Many variants exist depending on the scenario, for example problems involving viscosity may have $\nabla \cdot \mathbf{T} = \mu\nabla^2\mathbf{U}$, and problems involving multiphase fluids (in our case bubbles) may have $\rho = \rho_f - \rho_g$ to represent the phase dependent densities whilst surface tension effects are incorporated into $\mathbf{T}$. Hence after non-dimensionalisation the systems in bubble problems will often feature the following important dimensionless quantities:

The Reynolds number [15],

$$Re = \frac{\rho_f g^{1/2} R_0^{3/2}}{\mu_{ref}} \tag{11}$$

where ρ_f is the fluid density (gas density assumed to be zero), and R_0 and μ are characteristic scales for distance and viscosity used in the non-dimensionalisation. *Re* gives a measure of the importance of inertial versus viscosity forces, and as such $Re \approx 0$ corresponds to a relatively viscous fluid.

The Bond number [16] occurs in rising bubble problems

$$Bo = \frac{\rho_f g R_0^2}{\sigma} \tag{12}$$

since it compares buoyancy with surface tension.

For the collision of two bubbles with relative velocity $\mathbf{V}$, the Weber number [17]

$$We = \frac{\rho \mathbf{V}^2 R_{eq}}{\sigma} \tag{13}$$

is often used to measure inertia against surface tension. Here we define

$$R_{eq} = \frac{1}{2(R_1^{-1} + R_2^{-1})} \tag{14}$$

as the *equivalent radius* in the two-bubble system.

Another governing principle in fluid dynamics is the continuity equation

$$\frac{\partial \rho}{\partial t} = -\nabla \cdot (\rho \mathbf{U}) \tag{15}$$

which is used for conserved quantities, in this case density.

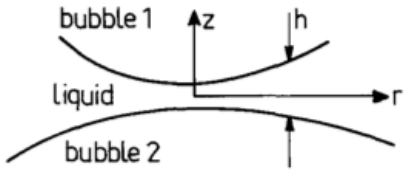

Figure 3: *Chesters and Hoffman's formulation of the binary collision system. Note how the bubbles' spherical symmetry has been exploited to reduce the dimensionality of the problem. Taken from [13].*

In [13] a binary bubble collision was modelled in coordinates centred at the point of contact (Fig. 3) in a gravity free environment. Writing (10) with pressure in terms of gas pressure and surface tensions across the boundaries of both bubbles and using the continuity equation to constrain the conservation of bubble volume, the equations were solved numerically for film thickness h to show that the minimum thickness occurs at some $r > 0$, indicating the formation of a dimple. This corroborates phase (2) of the coalescence description given at the start of this section, whereupon a small quantity of liquid becomes trapped at the interface.

By considering the energy required to deform the bubble surfaces in terms of *We*, and evaluating the time at which coalescence occurs, the pair showed that there exists a critical

Weber number, We_c, above which the bubbles will convert all their kinetic energy to free energy at the surface, arresting motion and causing the bubbles to bounce rather than coalesce. It was also shown that in the viscous case low Reynolds numbers correspond to a lower $\partial h/\partial t$ and thus a slower coalescence.

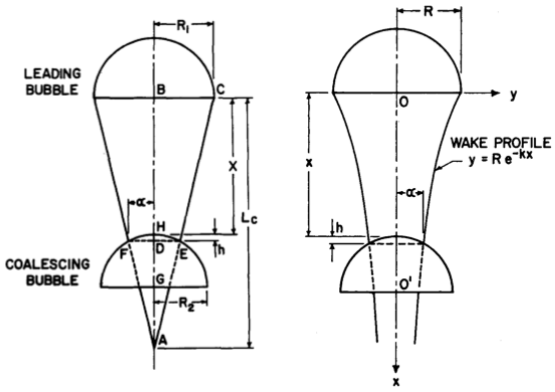

Figure 4: *The conical (left) and exponential (right) trailing wakes contemplated by de Nevers. Taken from [18].*

A different class of coalescence problem, that due to buoyancy, was first modelled by de Nevers and Wu [18]. It was observed that when two bubbles ascend in series the second one gains additional velocity from the upward-moving wake left by the first, eventually resulting in collision. Using hemispherical bubbles, the only two forces considered were buoyancy and drag, equilibrated for each bubble as

$$\left(\frac{2}{3}\pi R^3\right)\rho g = C_D\frac{\mathbf{U}^2}{2}A_p \qquad (16)$$

where C_D is the drag coefficient and A_p is the projected area of the leading edge. Two wake geometries were formulated; conical and exponential (Fig. 4). For the second bubble, drag was reduced by subtracting the area inside the first's wake from A_p, from which expressions for velocity and collision time were solved. The conical model has a finite wake, shown on the diagram to be of length L_c, so if the separation distance between bubbles is greater than this they will not coalesce. However the exponential model trails an infinite wake, and also happens to provide a (slightly) better fit to experimental data in glycerine. Interestingly, when testing with distilled water the authors chose to add sodium ethyl xanthate to reduce surface tension and promote coalescence. These simple models were unable to explain an observed further increase in velocity of both bubbles just prior to collision.

Considerably more complex was the buoyancy actuated model by Chen *et al.* [19], developed to provide 3D simulations over a range of Reynolds and Bond numbers to observe qualitative differences in the two-bubble dynamics.

The model was shown to match experimental footage with impressive accuracy (Fig. 5), though in this study the liquid jet formed behind the leading bubble at high Reynolds numbers was found to hinder coalescence, seemingly in contrast to the wake-accelerated model discussed previously. However, as in de Nevers' experiment, Chen's simulations perhaps unsurprisingly showed a lower σ value aided coalescence.

The system used 3D Navier-Stokes equations with viscosity and surface tension terms, and employed volume fraction function F, governed by the continuity equation, to represent the liquid and gas phase's separate density and viscosity properties, as well as the discontinuities at the fluid interface.

$$\rho(\mathbf{x},t) = F(\mathbf{x},t)\rho_f + [1 - F(\mathbf{x},t)\rho_g] \qquad (17)$$

$$\mu(\mathbf{x},t) = F(\mathbf{x},t)\mu_f + [1 - F(\mathbf{x},t)\mu_g] \qquad (18)$$

where $F = 0$ within the bubble, $F = 1$ within the liquid and $F \in (0,1)$ on the interface. F was also used to localise the surface tension as a volume force.

The system was solved over a cylindrical volume of stationary liquid, illustrated in Figure 5, for an initially spherical bubble resting along the central axis. The highly advanced numerical scheme was based on one developed in [20] and consisted of many sub-schemes. The Semi-Implicit Method for Pressure Linked Equations (SIMPLE) was used to link pressure and velocity, the Rhie-Chow interpolation method permitted edge dependent terms to be

used whilst allowing the mesh to remain collocated, a third-order upwind biased scheme was used for convection and second-order central differencing for diffusion, whilst a 27-point stencil was employed for surface-tension force linearisation. The transport functions (17) & (18) were solved with modified line-constant Volume of Fluid methods.

The author of this report made an attempt to understand this set of schemes and adapt them for modelling coalescence in decompressed tissue, but found the task hopelessly difficult, inspiring an examination of the next class of coalescence models.

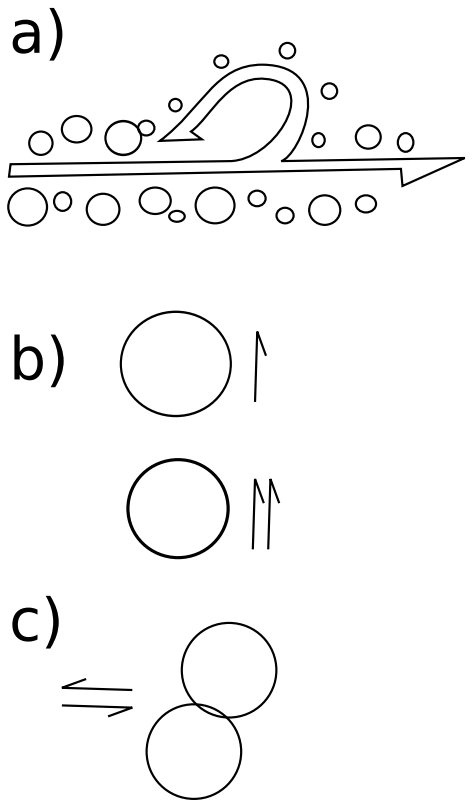

Figure 6: *Illustration of the three collision scenarios outlined in [21]. a) turbulence, b) buoyancy, c) laminar shear.*

Prince and Blanch [21] developed a probabilistic model for coalescence in large groups of bubbles, building on the work of Friedlander (1977). Observing that the coalescence rates were linked intrinsically with the collision rates, they categorised collision by type[2] into:

- Turbulence (Fig. 6a) - bubbles are propelled into one another by liquid eddy currents.
- Buoyancy (Fig. 6b) - already described.
- Laminar shear (Fig. 6c) - parallel streams of differing flow velocity could cause bubbles to interact with potential for coalescence. Currents need not be directly opposed, for example in pipe flow where the velocity is radially dependent.

They defined within a bubble mixture each type of collision rate between bubbles of radius i and j. Using buoyancy as an example:

$$\theta_{ij}^{B} = n_i n_j S_{ij}(u_{r_i} - u_{r_j}) \tag{19}$$

where u_{r_i} is the rise velocity, a function of volume and by implication R, and S is the collision cross-sectional area defined as

$$S_{ij} = \frac{\pi}{4}(r_i + r_j)^2 \tag{20}$$

Similar though more complicated rates were formulated for turbulence (θ^T) and laminar shear (θ^{LS}). Assuming the bubbles collide, they must remain in contact long enough for the film to rupture according to the film thinning equations developed by Chesters and Hoffman [13]. Defining the collision efficiency as

$$\lambda_{ij} = exp(t_{ij}/\tau_{ij}) \tag{21}$$

the authors totalled the three different collision types with coalescence efficiencies, then summed over all the possible discretised radii combinations to obtain the total coalescence rate:

$$\Gamma_T = \frac{1}{2}\Sigma_i\Sigma_j[\theta_{ij}^T + \theta_{ij}^B + \theta_{ij}^{LS}] \times \lambda_{ij} \tag{22}$$

Decoalescence or break-up was examined also, and both models were then shown to be able to describe experimental data.

[2]The author would like to point out that our research concerns a fourth type of collision - that driven by expansion.

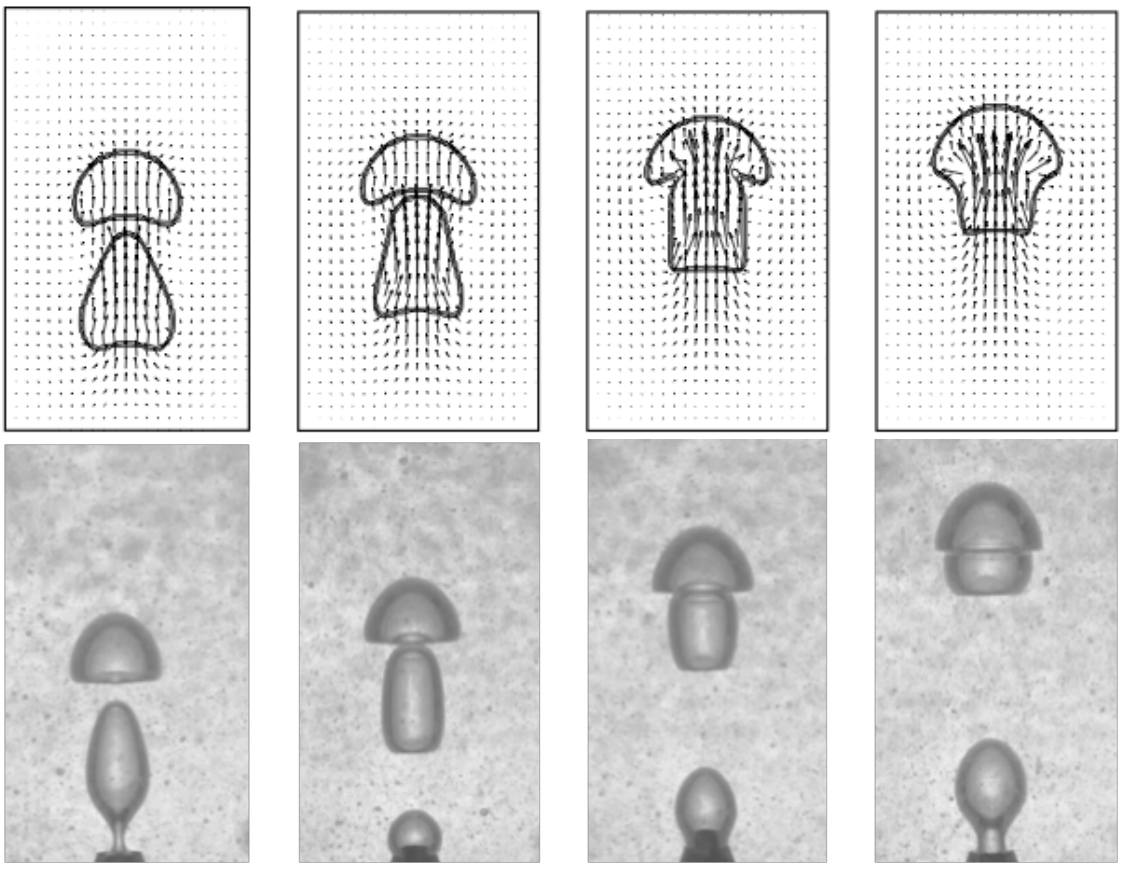

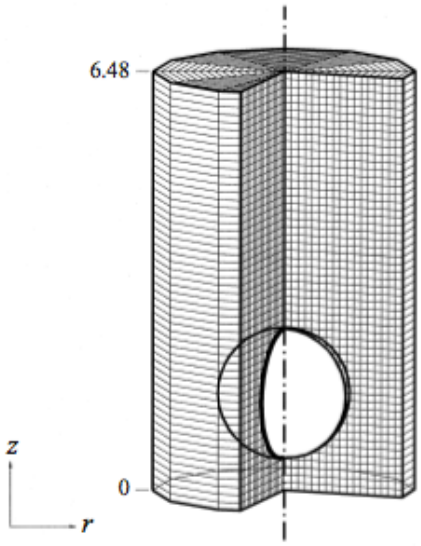

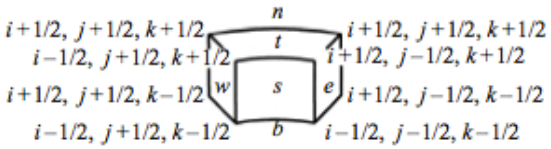

Figure 5: *Above: Comparison of model and experiment, adapted from [19]. Below: The cylindrical discretisation used for solving, taken from [20].*

The work of Prince and Blanch gave rise to a number of modified models from various authors, which are aggregated in a recently published paper by Nguyen *et al.* (2013) [12]. The group adapted Prince and Blanch's model to investigate the effect of bubbly flow inducing and suppressing turbulence, which as we have seen itself then influences the bubble dynamics.

All the coalescence models thus far have been Euler-Euler models in that both phases have been considered Eulerian fluids. Another recent paper by Mattson and Mahesh (2012) [22] used a probabilistic model but in an Euler-Lagrange system where the bubbles were considered hard spheres obeying Lagrangian particle system rules.

It has been noted in many works that the presence of electrolytes in solution reduces coalescence, with the foamy nature of seawater serving as a textbook example. In a letter to Nature [14] Craig *et al.* described an experiment where bubbles were passed through an illuminated water column and the escaping light recorded by a photodetector. The larger bubbles emerging from coalescence would allow maximum light through. The group then added increasing concentrations of NaCl and observed a logistic type decrease in transmission, indicating inhibition of coalescence. Systematically trying a number of different salts, the group then noticed not all of them had this effect, but fell into categories α and β such that anion cation pairings from the same category would inhibit coalescence, however alternate pairings had no effect whatsoever. The authors could provide no explanation for this phenomenon asides a possible mechanism through the (at the time of publishing) poorly understood long-range hydrophobic interaction.

In [23] Weissenborn and colleagues suggested the inhibition could also be a result of electrical repulsive forces or the Gibbs-Marangoni effect, concerning mass transfer between the fluid-bubble interface due to a surface tension gradient. They also pointed out a link between Craig's electrolyte pairings and oxygen solubility.

Interestingly, in another article [24] Craig remarks that the electrolyte concentration marking maximum coalescence inhibition coincides with the NaCl level in the human body, 1.1E-1M. He suggests that electrolytes *in vivo* play an essential role in preventing coalescence of ever-present microbubbles that would lead to DCS symptoms even at atmospheric conditions. The author of this report speculates that areas exhibiting the earliest symptoms of DCS could well have lower electrolyte concentrations than the rest of the body, though no study data has been yet found to corroborate this.

Salt inhibition was discussed in [21], with the suggested mechanism being immobilisation of the gas-liquid interface and subsequent increased required contact time t_{ij}. The critical electrolyte concentration was formulated as

$$c_t = 1.18 \left(\frac{B\sigma}{R} \right)^{1/2} R_g T \left(\frac{\partial \sigma}{\partial c} \right)^{-2} \tag{23}$$

where B is the retarded van der Waals coefficient.

Clearly a coalescence based model would do well to take salt concentrations into account, through (23) or otherwise.

To summarise the coalescence modelling section, it is clear that many different techniques have been used throughout the literature. All the models reviewed concern fluids in motion and some, particularly the model developed by Chen *et al.*, are very computationally intensive and far too detailed to be necessary in a diving algorithm. As the next section will show, bubbles do coalesce in tissue but not all the time, even when they start off touching, so more modelling is indeed required. The author would suggest using the Chesters and Hofman method, where relative velocity u is replaced by the relative expansion rate dR/dt to obtain pressure, distance and time ranges where coalescence is possible. Coalescence has been observed in more than two bubbles simultaneously [25], though this author has been unable to find any work on the modelling of such scenarios, so would suggest coalescing bubbles individually *in silico*.

Following coalescence of identical bubbles,

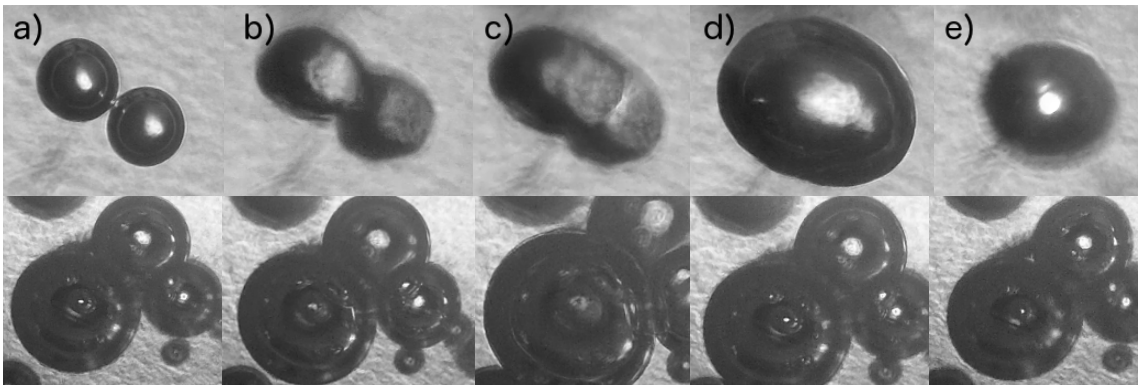

Figure 7: *Bubble coalescence in collagen hydrogel observed with (top) and without (bottom) success at UCL Institute of Orthopaedics and Musculoskeletal Science. Decompression cycle lasted 5 seconds.*

the resulting one would be centred on the point of contact ($r = 0$ in Figure 3) and have radius $2R$. For non equal bubble radii and approach velocities, the resulting radius would be

$$r_n = (r_1^3 + r_2^3)^{1/3} \tag{24}$$

though calculating the resulting centre has proved more difficult and seems to require solving numerically.

IV. Coalescence in collagen hydrogels

Collagen hydrogels have allowed the engineering of tissues containing cells and other biological structures in 3D configurations. They have proved very useful for studying bubbles under decompression due to being transparent, firm enough to hold their contents in a fixed position and yet still respond well to pressure changes in a vacuum chamber, and relatively simple to make given their biological semblance.

The hydrogel consists of intact collagen fibrils, essential media containing salt concentrations, pH indicator, and NaOH to neutralise the acetic acid used to extract and store the fibrils [26]. By shaking the mixture before setting at 37°C, the hydrogel can be set with micro bubbles scattered throughout.

In Figure 7, stills from videos taken at UCL Stanmore Campus illustrate the fact bubbles may coalesce in tissue under depressurisation, but may also just expand even in close contact whilst remaining separate. An experiment was attempted to examine the effect of NaCl concentration on coalescence. The results were not in line with those reported in the literature, so the experiment almost certainly contained mistakes, however the details shall be included here for completeness.

Bubbly hydrogels were produced with essential media NaCl concentrations 0, 1.5, 4 & 10 Mols/l. 3 gels of each concentration were made so the experiment could be repeated. Photos were then taken at 3 random locations on each of the 12 gels before and after decompression to 0.1 atm followed by return to ambient pressure, the theory being that the average bubble number would decrease following coalescence, and a relationship should emerge with NaCl content. Photos of an Optik Labor 0,0025mm^2 cell sizer were taken also to provide scale reference.

Bubble counting was automated using Matlab's image processing functions, most notably 'imfindcircles'. Bubble diameters ranged from 0.02mm - 0.96mm. Results are shown in Figure 8. Surprisingly, many of the bubble counts seemed to increase following decompression, quite the opposite of what we were expecting. Note that at no point during decompression was decoalescence observed. The inconclusive results could be down to a number of factors.

First the method of obtaining bubble count by averaging over 3 photos could be at fault. Reliable results would need very large numbers to constitute a representative average, especially given that reported densities can be as high as 10^4 bubbles/ml [5]. Additionally the mixing process for introducing bubbles was carried out by a human and thus has none of the consistency of the bubble apparatus described in the literature review section of this report. Finally it is quite possible that the low pressure environment was not maintained for long enough. Much of the bubble modelling literature has placed emphasis on the time taken for the liquid film to drain during coalescence. Granted the times are often of order milliseconds, but the conditions have been wildly different due to the viscous nature of the medium we used, and the inflation based collisions.

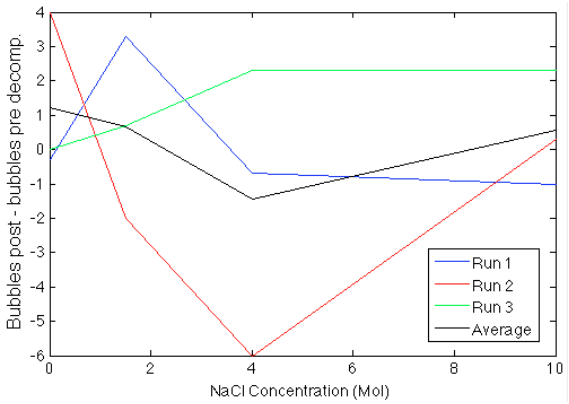

Figure 8: *NaCl concentration versus change in bubble numbers following decompression*

References

[1] Chappell, Michael. Modelling and Measurement of Bubbles in Decompression Sickness. Diss. University of Oxford, 2006.

[2] Francis, T. James R., and D. J. Smith. Describing Decompression Illness. Undersea and Hyperbaric Medical Society, Inc., 1991.

[3] Nagle, Fintan S. "Techniques for in vivo observation of the pathophysiology of DCS."

[4] Kindwall, E. P., et al. "Nitrogen elimination in man during decompression." Undersea biomedical research 2.4 (1975): 285.

[5] O'Brien, J.P. "Notes on decompression model." UCL Mathematics (2012).

[6] Srinivasan, R. Srini, Wayne A. Gerth, and Michael R. Powell. "Mathematical models of diffusion-limited gas bubble dynamics in tissue." Journal of Applied Physiology 86.2 (1999): 732-741.

[7] Srinivasan, R. Srini, Wayne A. Gerth, and Michael R. Powell. "A mathematical model of diffusion-limited gas bubble dynamics in tissue with varying diffusion region thickness." Respiration physiology 123.1 (2000): 153-164.

[8] Srinivasan, R. Srini, Wayne A. Gerth, and Michael R. Powell. "Mathematical model of diffusion-limited gas bubble dynamics in unstirred tissue with finite volume." Annals of biomedical engineering 30.2 (2002): 232-246.

[9] Srinivasan, R. Srini, Wayne A. Gerth, and Michael R. Powell. "Mathematical model of diffusion-limited evolution of multiple gas bubbles in tissue." Annals of Biomedical Engineering 31.4 (2003): 471-481.

[10] Daniels, S., J. M. Davies, W. D. Paton and E. B. Smith (1980). "The Detection of Gas Bubbles in Guinea-Pigs after Decompression from Air Saturation Dives Using Ultrasonic Imaging." Journal of Physiology (London) 308(1): 369-383.

[11] Lever, M. J., et al. "Experiments on the genesis of bubbles as a result of rapid decompression." The Journal of Physiology 184.4 (1966): 964-969.

[12] Nguyen, V.T., Song, C.H., Bae B.U., and Euh, D.J. "Modeling of bubble coalescence

and break-up considering turbulent suppression phenomena in bubbly two-phase flow" International Journal of Multiphase Flow 54 (2013): 31-42.

[13] Chesters, A. K., and G. Hofman. "Bubble coalescence in pure liquids." Applied Scientific Research 38.1 (1982): 353-361.

[14] Craig, V. S. J., B. W. Ninham, and R. M. Pashley. "Effect of electrolytes on bubble coalescence." Nature 364.6435 (1993): 317-319.

[15] Brennen, Christopher Earls. Cavitation and bubble dynamics. Vol. 44. Oxford University Press on Demand, 1995.

[16] Zapryanov, Z., and S. Tabakova. Dynamics of bubbles, drops and rigid particles. Vol. 50. Springer, 1998.

[17] Duineveld, P. C. "Bouncing and coalescence of bubble pairs rising at high Reynolds number in pure water or aqueous surfactant solutions." Applied scientific research 58.1-4 (1997): 409-439.

[18] de Nevers, Noel, and Jen?Liang Wu. "Bubble coalescence in viscous fluids." AIChE Journal 17.1 (1971): 182-186.

[19] Chen, Li, Yuguo Li, and Richard Manasseh. "The coalescence of bubbles-a numerical study." Third International Conference on Multiphase Flow, ICMF. Vol. 98. 1998.

[20] Chen, Li, et al. "The development of a bubble rising in a viscous liquid." Journal of Fluid Mechanics 387 (1999): 61-96.

[21] Prince, Michael J., and Harvey W. Blanch. "Bubble coalescence and break?up in air?sparged bubble columns." AIChE Journal 36.10 (1990): 1485-1499.

[22] Mattson, M. D., and Krishnan Mahesh. "A one-way coupled, EulerÐLagrangian simulation of bubble coalescence in a turbulent pipe flow." International Journal of Multiphase Flow 40 (2012): 68-82.

[23] Weissenborn, Peter K., and Robert J. Pugh. "Surface tension and bubble coalescence phenomena of aqueous solutions of electrolytes." Langmuir 11.5 (1995): 1422-1426.

[24] Craig, Vincent SJ, Barry W. Ninham, and Richard M. Pashley. "The effect of electrolytes on bubble coalescence in water." The Journal of Physical Chemistry 97.39 (1993): 10192-10197.

[25] Postema, Michiel, et al. "Ultrasound-induced microbubble coalescence." Ultrasound in medicine & biology 30.10 (2004): 1337-1344.

[26] Cheemer, U. "3D collagen biomatrix development." UCL lecture notes (2012).